

David A. MacLucas · Beric W. Skews · Harald Kleine

High-speed imaging of shock wave focusing in concave profiles using shearing interferometry and direction-indicating colour schlieren

Received: 30 September 2014 / Revised: 16 November 2014 / Accepted: 30 November 2014 / Published online: 27 December 2014
© The Visualization Society of Japan 2014

Abstract In this study both qualitative and quantitative flow visualization techniques are used to examine the complex flow field developed during the interaction of a plane shock wave with a compound profile. Shearing interferometry and direction-indicating colour schlieren are implemented in conjunction with high-speed time-resolved imaging. Comparisons between the results provided by the two flow visualization systems are made at incident shock strengths of Mach 1.28 and Mach 1.35. The results from both systems indicate the complex nature of the transient compression and expansion systems developed during the interaction behind the various shock fronts. The direction-indicating results prove valuable in eliminating the ambiguity with respect to the sign of the high-order fringes found in the shearing interferometry results.

Keywords Shock focusing · Flow visualization · High speed flows · Shearing interferometry · Direction-indicating colour schlieren

1 Introduction

Analysis of shock wave interactions remains predominantly experimentally-based. Flow visualisation techniques are used to capture the interaction, thereby providing the means to examine complex shock wave behaviour as seen in the topic of interest of this work: shock wave focusing. The preeminent study in shock wave focusing, by Sturtevant and Kulkarny (1976), relied on single-image shadowgraphy to capture the interaction of plane shock wave with various parabolic profiles. Shadowgraphy is valuable for visualizing the shock waves and shear layers in the flow field but as it is sensitive only to the second derivative of density, shadowgrams cannot be used for quantitative evaluation of the density distribution in the flow. As a result, the authors could not observe the development of various expansive and compressive fields which are an important part of the shock wave focusing process. Improvements of time-resolved high-speed imaging, used in combination with density-based flow visualization techniques, have provided an impetus to revisit the interaction of a plane shock wave in air with a concave profile. The ability to track various flow features, frame-by-frame in high resolution, allows one to examine the progression of highly transient flow features developed within the reflector, and the refinement of visualisation techniques permits observation of less pronounced flow structures that would remain unnoticed in less sensitive systems. This work aims to

D. A. MacLucas (✉) · B. W. Skews
Flow Research Unit, School of Mechanical, Industrial and Aeronautical Engineering, University of the Witwatersrand,
Johannesburg 2050, South Africa
E-mail: dmaclucas@csir.co.za
Tel.: +27 12 841 3574

H. Kleine
University of the New South Wales, School of Engineering and IT, Canberra, ACT 2600, Australia

demonstrate the significant benefits of using shearing interferometry and direction-indicating colour schlieren in the analysis of two-dimensional shock wave interaction cases. Specifically, these techniques are used to visualize the complex flow field developed during the interaction of a plane shock wave in air with a specially developed compound profile.

2 Apparatus

2.1 Experimental setup

Experiments were conducted in a conventional diaphragm-operated air-driven shock tube with a 150 mm by 75 mm test section (low pressure part length: 5.3 m). A single compound profile was tested as illustrated below in Fig. 1. The profile consists of a weighted catenary base $x = 1 - \cosh(5y)$ fitted with a parabolic inlet $(y + 0.003) = -24.7515x^2$. The compound profile was designed to evaluate the effects of a convex inlet on the shock focusing process. However, for the purposes of this work only the application of the flow visualization techniques to this complex flow are discussed. The test piece was fitted into the shock tube such that a 5 mm gap existed between both the top and bottom walls of the tunnel (see Fig. 1b). This was done in order to eliminate possible effects the shock tube walls and the boundary layers developing on them could have on the focusing process. The flow visualization techniques implemented were based on a combination of the requirements to resolve specific flow features and to explore the capabilities of quantitative systems. The arrangements of the optical components used for the shearing interferometry system and the direction-indicating colour schlieren system are illustrated below in Fig. 2.

The system has two schlieren mirrors with a 240 mm free diameter and 2,624 mm focal length in a Z-type configuration. Due to the off-axis arrangement of the mirrors, a cylindrical lens is used to minimize the astigmatic difference between foci in the sagittal and meridional planes at the second mirror (Prescott and Gayhart 1951). This correction is required for the direction-indicating colour schlieren method and is also useful for the shearing interferometry setup. Coma is eliminated by using mirrors of equal focal length and ensuring the angles between the trunk of the Z and its branches are equal opposite. The high-speed camera used for these tests was a prototype developed by NHK (Ohtake et al. 2006) and has the capability to record colour videos at 1,000 000 frames-per-second (fps) at a resolution of 720 (width) \times 410 (height) pixels. The camera uses a specialised CCD sensor developed by Etoh et al. (2002) for time-resolved high-speed imaging. The high frame rate, high sensitivity and good image resolution make the NHK camera ideal

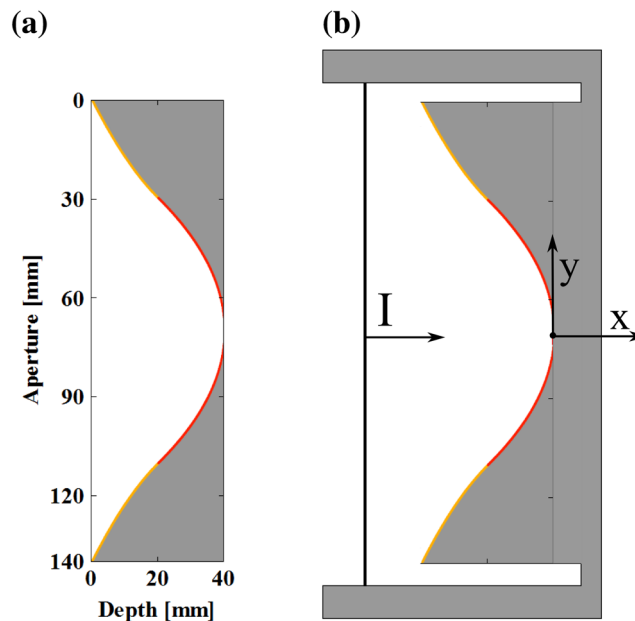


Fig. 1 Weighted catenary–parabolic compound profile used for experimental testing. **a** Dimensions of profile (*red contour* weighted catenary, *yellow contour* parabolic). **b** Experimental arrangement of the profile in the test section

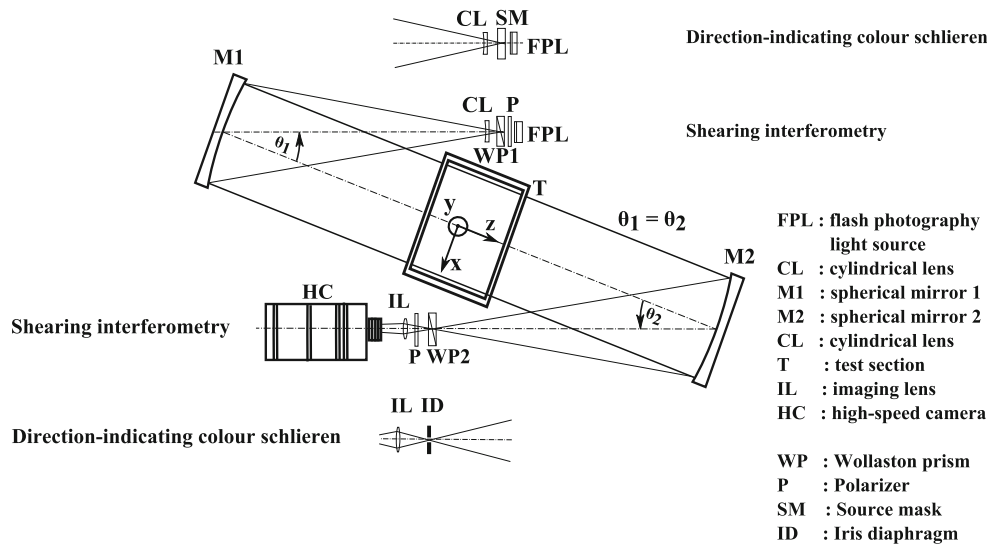


Fig. 2 Flow visualization setup used for the shearing interferometry and direction-indicating colour schlieren systems. Figure adapted from (Kleine 2001). Note co-ordinate axes where y is measured perpendicular to the page

for high-speed photography of transient phenomena such as the cavity flows observed here. Both the camera and the flash lamp were triggered via a pressure transducer positioned upstream of the test section.

2.2 Shearing interferometry

Shearing interferometry yields both qualitative and quantitative information about the flow field under study. The system is also referred to as a differential schlieren system owing to the similarities to a schlieren system both with respect to setup and results. The beam separation or shear d is generated by a Wollaston prism. The shear can be determined as $d = f_2 \cdot \varepsilon$ where f_2 is the focal length of mirror 2 and ε is the beam divergence angle of the Wollaston prism. When the initially separated beams are recombined and allowed to interfere, the resulting fringes represent areas of constant density gradient, in the direction of the shear (Merzkirch 1987).

The setup of the Wollaston prism interferometer is illustrated above in Fig. 2. Since the system was operated using a polychromatic light source, the fringe order is equivalent to a colour coded phase shift. The phase shift associated with each colour fringe is tabulated in handbooks, e.g. Oertel and Oertel (1989). The system used the Z configuration arrangement where a Wollaston prism (with a separation angle ε of 1 arc minute) is placed at the focal point of the second mirror. The spatial coherence of the light provided by the flash lamp was improved by placing another Wollaston prism in the focal spot of the first mirror (Merzkirch 1987).

The prism at the focal point of the second mirror acts as a shearing element, by placing beams separated by distance d in the test section on the same optical path. Note that the two beams leaving the prism are polarized orthogonal to each other, according to the polarization axes of the Wollaston prism. A polarizer placed behind the prism, rotated at 45° to the polarization axes of the prism, permits interference of the two beams by ensuring that both rays have an equal direction of polarization. The polarizer placed ahead of focal point of the first mirror ensures equal light intensity in both polarization axes of the prism (Kleine 2001). Since the system produces two parallel beams through the test-section, discontinuities (body contours, shocks and contact surfaces) in the direction of the shear (here: x direction) produce a double image which in the current setup is approximately 5 pixels wide ($d = 0.764 \text{ mm} \leq 5 \text{ pixels}$). Therefore, interpretation of flow features and fringes adjacent to such discontinuities should be done with care since the spatial resolution of these features will be compromised. Note that flow features smaller than the shear cannot be adequately resolved.

The calibration of the system was achieved by following the procedure outlined by (Kleine 2001). The system was operated in the infinite fringe mode, where the 'sky blue' fringe was selected as the background and reference fringe for all tests using shearing interferometry. A plano-convex lens of large focal length (10.27 m) was imaged in the test section revealing a range of vertical fringes where, in infinite fringe mode,

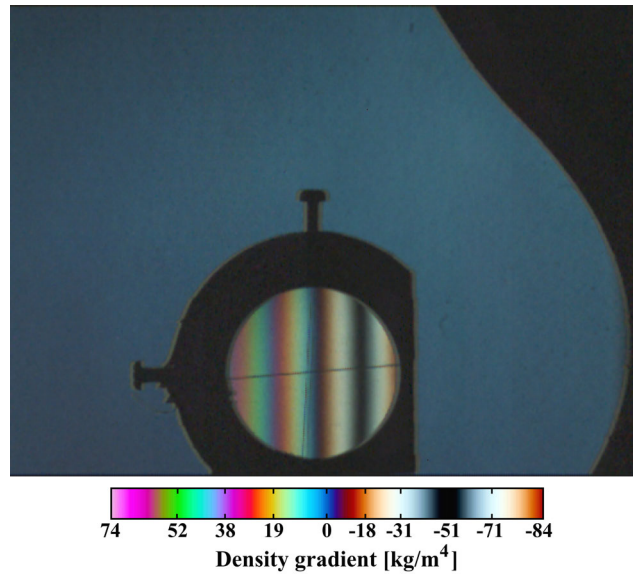


Fig. 3 Calibration image for the shearing interferometry setup. A guide to the correlation between density gradient magnitude and fringe colour for a few fringes are shown below the calibration image. This guide also provides the calibrated measurement range for the shearing interferometry system

the centre fringe corresponds to the colour of the background. The calibration image for the compound profile is shown above in Fig. 3 (note that the Wollaston prisms are aligned to measure horizontal density gradients). Since the fringes are symmetrical about the zero-order (black) fringe, the sign of the density gradient component can become ambiguous (Kleine 2001). To reduce this effect, the aforementioned sky blue higher-order fringe was chosen as background representing a density gradient of zero. In addition, schlieren results are used to clarify the sign of the gradient in ambiguous cases.

2.3 Direction indicating colour schlieren

The direction-indicating colour schlieren technique, based on the dissection technique devised by Cords (1968), was developed by Settles (1970 and 1985) and later applied to shock tube flows by Kleine and Grönig (1991). This novel system indicates the direction of the density gradient of the visualized flow field by a specific colour. Colour systems are advantageous since changes in colour are easier to distinguish than monochrome illumination changes, however they are less sensitive than an equivalent monochrome system (Kleine 2001). A colour source mask (see Fig. 4a) is introduced at the focal point of the first schlieren mirror. The colour mask uses the three primary colours, arranged in near 120° intervals in an elliptical pattern (the elliptical shape is a consequence of the necessary astigmatism correction in the setup; Kleine 2001) giving the system uniform omnidirectional sensitivity. The correlation between colour and the direction of the density gradient that the colour represents, was established by taking a calibration image of the aforementioned high-focal length plano-convex lens in the test section and is shown below in Fig. 4b. Note that the direction of a positive density gradient, for each direction, lies along a radial line pointed toward the centre of the circle (see Fig. 4b). Cut-off was achieved by placing an iris diaphragm at the focal point of the second schlieren mirror and adjusting its aperture to correspond to the inner diameter of the colour mask (Settles 1985; Kleine and Grönig 1991; Kleine 2001).

3 General features of the interaction

Results from two tests at two different incident shock strengths using both shearing interferometry and direction-indicating schlieren are compared in the results section below. The shearing interferometry test was conducted at an incident shock strength of $Mach = 1.35$ while the incident shock Mach number was $M = 1.28$ in the direction-indicating colour schlieren test. Though the incident shock strengths differ, the results are qualitatively identical. In both tests, sets of images were captured at a frame rate of 180,000

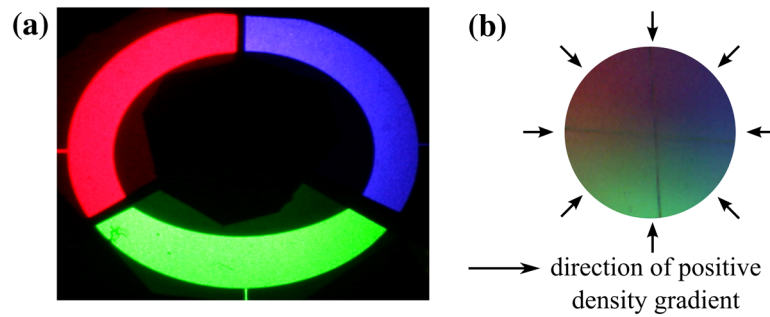


Fig. 4 **a** Colour source mask (SM) used for the direction-indicating schlieren. **b** Calibration image annotated with the positive sense for the density gradient

frames per second, i.e. 180 kfps. The exposure time for each frame is $0.69 \mu\text{s}$. Note that due to the opening of the diaphragm, transverse waves are generated that trail the incident shock wave, and those waves are more pronounced with increasing incident shock strength. These waves distort the fringes and colours in an area of interest by inducing an additional phase shift or refraction of the light in the affected area. Transverse waves are easily discerned in the images below, since they are not symmetrical about the centre line axis of the compound profile. In spite of their occasionally prominent appearance, these transverse waves are typically only weak disturbances, as is shown, for example, by the usually minute amount of fringe distortion they cause on the shearing interferometry results. Furthermore, one can determine from consecutive images that these waves propagate at the post-shock sound speed with respect to the post-shock flow, so they can be considered as Mach waves.

3.1 Initial engagement

The initial engagement of the plane shock wave with the profile wall results in a reflection R of the incident shock wave I as seen in images a1 and a2 of Fig. 5. The ability of both systems to resolve the various primary shock waves in the transient flow field is evident. In addition, the high sensitivity of both systems is apparent where weak transverse waves are clearly resolved in both sets of tests (see Fig. 5) along with weak waves like the compression wave C (see images a1 and a2 of Fig. 5); the compression wave C arises from shock diffraction at the profile tip due to the gap between the profile and the tunnel wall. The high sensitivity of both systems, in combination with the time-resolved imaging, permits the tracking of even minute disturbances in the flow. In the setup used, the shearing interferometry system is more sensitive, but only in the direction of shear. Images a1, b1 and c1 of Fig. 5 indicate numerous transverse waves, which are not resolved in the direction-indicating schlieren results of images a2, b2 and c2 in Fig. 5. This is a consequence of the hue changes due to density gradients being more gradual in the colour schlieren system, which primarily operates with three primary and three secondary colours, whereas the wide interference colour range makes it possible that even small phase shifts lead to clearly distinguishable colour differences in the used shearing interferometer. The ability of the shearing interferometry to resolve these weak waves, along with quantifying their effect is quite advantageous in establishing their influence on the flow field of interest. Image c1 of Fig. 5 illustrates that the additional phase shift generated, when the most prominent transverse wave interacts with the reflected shock wave R, is relatively small. When this wave interacts with the compressive system adjacent to R (see Sect. 3.2) the fringe order decreases (by comparing fringe pattern adjacent to the wave) and represents a negative density gradient of $(\partial\rho/\partial x) \leq -18 \text{ kg/m}^4$. The effect of these waves on the flow field of interest is minimal since no variation in shock wave reflection type is observed. In addition, no permanent variations of the compressive/expansive fields occur which can be verified by comparing the flow on either side of the profile centre line as the inclined transverse waves affect each side of the reflector differently.

Along with identifying the various shock waves developed in this interaction both systems also provide valuable information on the flow behind the shock waves. Images a1 and a2 of Fig. 5 indicate highly non-uniform flow behind the reflected shock wave R as seen along its length. At the intersection of the reflected wave R and the incident shock wave I, a red patch (Fig. 5a2) is present between the wall and the reflection point. However, this change in density behind R dissipates away from the wall and further up R where the background colour is present. Thereafter, at the intersection of the compression wave C and the reflected

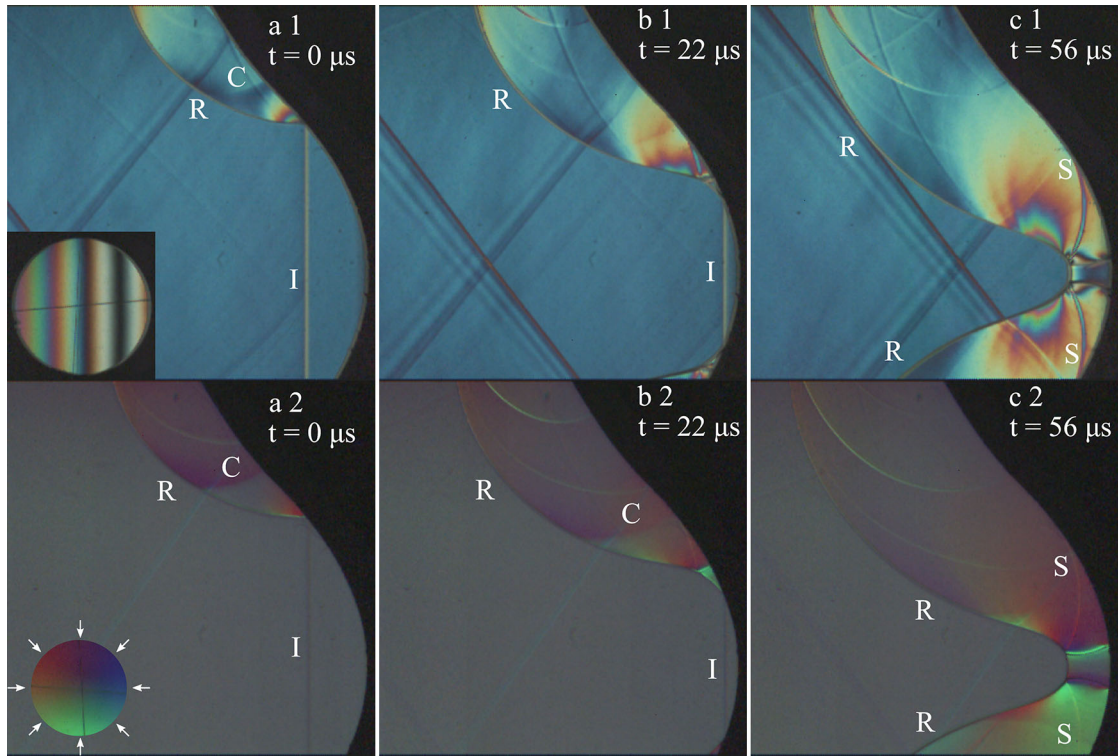


Fig. 5 Visualisation of the initial engagement of a planar shock with the compound profile; time-resolved images taken with 180 kfps. Exposure time for each frame: $0.69 \mu\text{s}$. Image time stamps for both sets of results are measured relative to images a1 and a2 respectively. *Top row* shearing interferometry, initial shock Mach number $M = 1.35$. *Bottom row* direction-indicating schlieren, initial shock Mach number $M = 1.28$

shock wave R, the area behind R and C is coloured purple. Using the colour correlation diagram in image a2 of Fig. 5, it is clear that the red patch seen at the reflection point of R and I indicates an expansion. This is also true of the area behind C and further up R, where the direction for increasing density gradient indicates an expansion behind R and C. However, the red patch adjacent to R, developed along the section of R moving into the oncoming flow, indicates a compressive region behind this section of R. Thus from a single image, a vast amount of information can be extracted about not only the shock waves but also the nature of the flow field behind these shock waves.

3.2 Gas dynamic focus

The images of Fig. 6 illustrate the complex process of gas dynamic focus, which starts in images a1 and a2 and concludes in images c1 and c2. As mentioned earlier, the direction-indicating schlieren is most useful for identifying the nature of the flow behind the curved shock waves developed in this interaction, while the shearing interferometry is valuable in quantifying the density gradients behind the shock waves. Take for instance image a1 of Fig. 6, where high order fringes are seen adjacent to the reflected shock wave M and the reflected shock wave R. However, the sign of the gradients is ambiguous since these fringes could occur on either side of the background fringe. In this instance, direction-indicating schlieren (Image a2 of Fig. 6) produces red and green patches on both sides of the symmetry plane adjacent to M and R. With the aid of the colour correlation diagram (image a2 of Fig. 6), these patches indicate that the density increases away from R. This is clear evidence of a compressive region. In this manner the two flow visualization systems are complimentary allowing not only the direction of the density gradient to be determined but also the variation and strength of the compressive/expansion region behind the shock waves. The fringes in this compression exceed the positive calibration range (matt purple fringe in the density gradient correlation guide in Fig. 3) indicating the horizontal density gradients exceed $(\partial\rho/\partial x) > 74 \text{ kg/m}^4$. Clearly, there are significant density gradients in these compressive areas. The development and evolution of this compressive region, during the focus process, can be viewed across the images a1, b1 and c1 of Fig. 6.

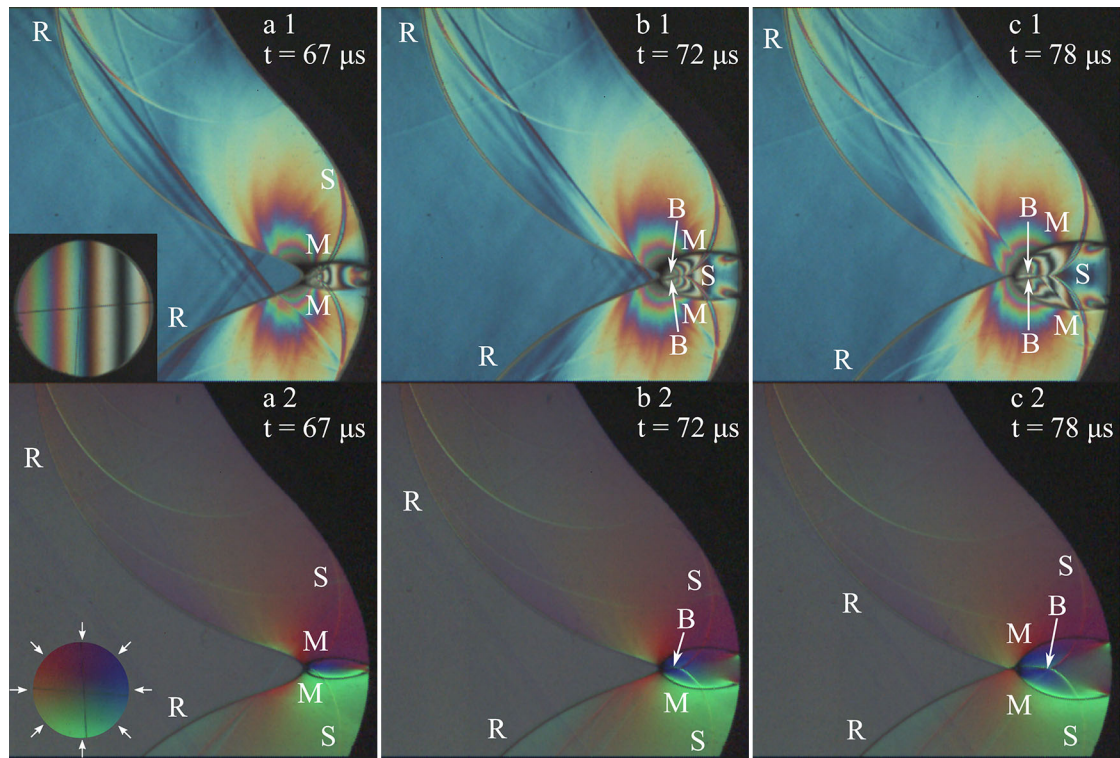


Fig. 6 Visualisation of the development of gas dynamic focus during the interaction of a plane shock wave with the compound profile; time-resolved images taken at 180 kfps. Exposure time for each frame: $0.69 \mu\text{s}$. *Top row* shearing interferometry, incident shock Mach number $M = 1.35$. *Bottom row* direction-indicating colour schlieren, incident shock Mach number $M = 1.28$

3.3 Post-focus behaviour

The images of Fig. 7 illustrate the post-focus wave behaviour, where the focus process is complete and the shock system developed at focus moves away from the base of the profile. These images once again illustrate the complex nature of the flow field behind the various shock waves. Both flow visualization systems are most useful in identifying regions of flow with no density changes. The area between the shear layers S and the base of the profile wall are coloured with the background fringe (image b1 of Fig. 7) indicating an area of zero density gradient and, in this case, most likely zero velocity. This result is corroborated by the schlieren results (image b2 of Fig. 7) where the background colour is found in the same area.

The development and evolution of a jet developed along the shear layers B is illustrated in both sets of results. Two opposing vortices can be seen on either side of the centre line shear layers B (images b1 and b2 of Fig. 7). The structure of these vortices is not entirely clear from the shearing interferometry results (images b1 and c1) since significant density changes occur in a confined area, which leads to the superposition of numerous fringes. However, the direction-indicating schlieren results (images b2 and c2 of Fig. 7) clearly show the shape and structure of the vortices. These vortices can be seen rolling up into the shear layers B found on either side of the two vortices (images b2 and c2 of Fig. 7). These images also show purple and green patches on either side of the centre line shear layer B. These patches indicate that the air density increases toward this centre line shear layer.

The shearing interferometry results (images b1 and c1 of Fig. 7) show a V-shaped brown patch along the centre line shear layer B. This fringe provides an unambiguous indication of an expansion in this area. In addition, these images also show that low magnitude expansions are developed on either side of the centre line shear layer B (brown fringes indicate gradients of $(\partial\rho/\partial x) = -18 \text{ kg/m}^4$) and along the shear layers S by the brown/blue areas ($-18 < (\partial\rho/\partial x) < -6 \text{ kg/m}^4$). The density gradient distribution in these areas changes as the main shock wave system moves away from the base of the profile. This is indicated by the fringes changing from brown/blue colour to a dark blue/indigo colour ($(\partial\rho/\partial x) = -6 \text{ kg/m}^4$). These are very

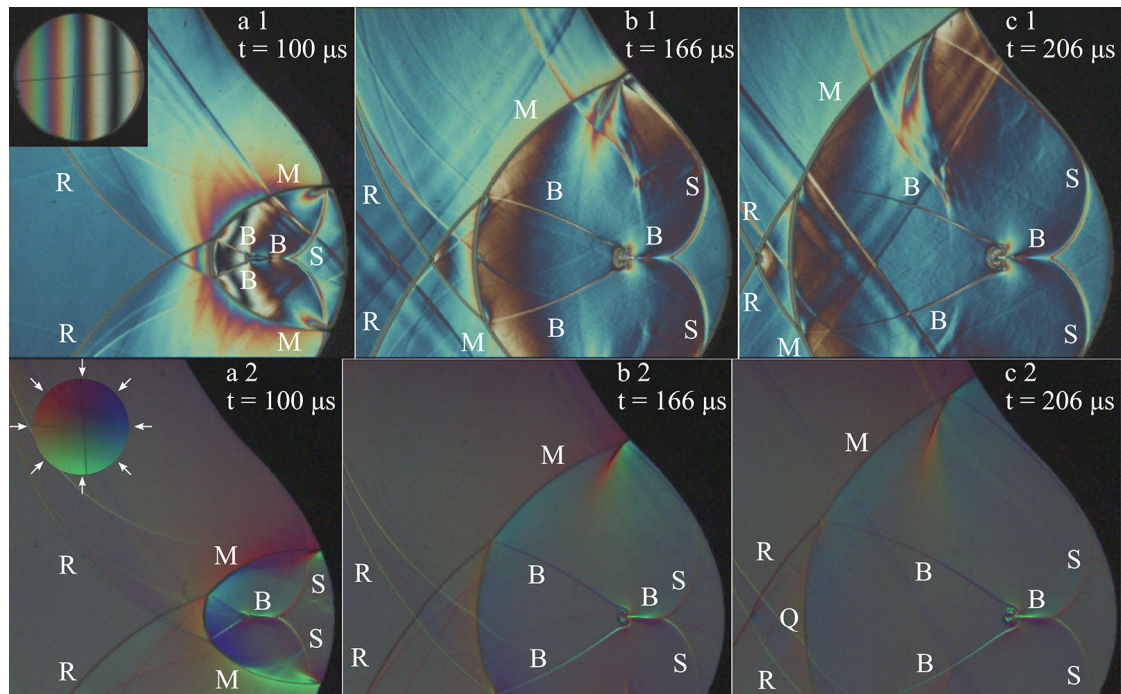


Fig. 7 Visualisation of the post-focus shock wave behaviour during the interaction of a plane shock wave with the compound profile; time-resolved images taken at 180 kfps. Exposure time for each frame: $0.69 \mu\text{s}$. *Top row* shearing interferometry, incident shock Mach number $M = 1.35$. *Bottom row* direction-indicating colour schlieren, incident shock Mach number $M = 1.28$

subtle changes in fringe order, only visible due to the large area which the fringes occupy. Note that the list of colour fringes, given, e.g. by Oertel and Oertel (1989), indicate that a shearing interferometry system is capable of producing very fine nuances in fringe colour. These are not always resolved in the calibration image and in the results themselves (Kleine 2001) as these nuances represent minuscule density gradients. This is especially true in confined areas with strong density changes.

4 Conclusions

The results from both the shearing interferometry and the direction-indicating schlieren have proven highly valuable in analysing a complex transient flow field. The direction-indicating schlieren method has permitted the discernment of the numerous compression and expansion systems in the flow. The shearing interferometry setup has been useful in quantifying the strength of these compression and expansion systems, along with the sign of the density gradient, in instances when the resulting fringes occurred between the zero-order fringe and the reference fringes. For fringes outside of this range, the direction-indicating schlieren proved useful in removing the sign ambiguity. The shearing interferometry system also proved most useful in resolving unintended transverse waves in the flow field and quantifying their effect on the flow field of interest. Both techniques, in particular their combined use for the same gas dynamic scenario, have provided an unprecedented description of the flow without resorting to numerical techniques. These systems are highly recommended for the analysis of highly transient two-dimensional flow fields.

Acknowledgments The authors wish to extend a special thanks to Prof. T. G. Etoh and Prof. K. Takehara of Kinki University, Osaka, Japan, for the use of their exceptional high-speed camera which made this work possible. The authors also wish to thank both the South African National Research Foundation for the KIC travel grant along with project Fluxion for their financial support during the first author's post-graduate studies. The first author is also in deep gratitude to the CSIR for providing the time necessary to complete this work.

References

- Cords PH (1968) A high resolution, high sensitivity color schlieren method. *SPIE J* 6:85–88
- Etoh TG, Poggemann D, Ruckelshausen A, Theuwissen A, Kreider G, Folkerts H-O, Mutoh H, Kondo Y, Maruno H, Takubo K, Soya H, Takehara K, Okinaka T, Takano Y, Reisinger T, Lohmann C (2002) A CCD image sensor of 1 Mframes/s for continuous imaging capturing of 103 frames. In: Technical digest of international solid state circuit conference. IEEE 0-7803-7335-9/02, pp 45–48
- Kleine H (2001) Measurement techniques and diagnostics: flow visualization. In: Ben-Dor G, Igra O, Elperin T (eds) *Handbook of shock waves*. Academic Press, San Diego, pp 685–738
- Kleine H, Grönig H (1991) Color schlieren methods in shock wave research. *Shock Waves* 1:51–63
- Merzkirch W (1987) *Flow visualization*, 2nd edn. Florida Academic Press, Orlando
- Oertel H Sr., Oertel H Jr. (1989) *Optische strömungsmeßtechnik*. Karlsruhe, G. Braun
- Ohtake H, Hayashida T, Kitamura K, Arai T, Yonai J, Tanioka K, Maruyama H, Etoh TG (2006) 300,000-pixel ultrahigh-speed high-sensitivity CCD and single-chip color camera mounting this CCD. *NHK Broadcast Technol* 28:2–9
- Prescott R, Gayhart EL (1951) A method of correction of astigmatism in schlieren systems. *J Aeronaut Sci* 18:69
- Settles GS (1970) A direction-indicating color schlieren system. *AIAA J* 8:2282–2284
- Settles GS (1985) Colour-coding schlieren techniques for the optical study of heat and fluid flow. *Int J Heat Fluid Flow* 6:3–15
- Sturtevant B, Kulkarny VA (1976) The focusing of weak shock waves. *J Fluid Mech* 73(4):651–671